Carboxylated chalcone and benzaldehyde derivatives of triosmium carbonyl clusters: Synthesis, characterization and biological activity towards MCF-7 cells

---

Abstract

The activated cluster $Os_3(CO)_{10}(CH_3CN)_2$ (**1**) reacts readily with a number of carboxylated chalcones and benzaldehydes (**2a**–**j**) to afford products with the general formula $Os_3(CO)_{10}(\mu\text{-}H)(\mu\text{-}O_2CR)$ (**3a**–**j**). The structures of all the novel clusters have been characterized by IR and ^{1}H NMR spectroscopy, as well as mass spectrometry and elemental analysis. Single-crystal X-ray diffraction analysis has also been carried out for one of the carboxylated chalcones and two of the derivatized clusters. The activity of some of the derivatized clusters against the ER+ breast carcinoma MCF-7 cancer cell line has also been evaluated.

Keywords: Benzaldehyde; Carboxylato; Chalcone; Ferrocene; Osmium cluster

1. Introduction

There is continued interest in harnessing the highly robust osmium carbonyl cluster cores for various areas of study and application. One area pertains to the reactivity and transformation of organic moieties tethered to osmium clusters, with carborane cages [1] and diphosphines [2] being the subject of recent investigations. Another encompasses bio-sensing and bio-imaging; the carbonyl ligands exhibit characteristic vibrational frequencies in the 1650–2200 cm^{-1} range, which are unobscured by other organic functional groups, complementing the highly stable metal cores for utilization in biological systems [3]. The conjugation of biologically active molecules to osmium carbonyl clusters is thus of interest for the development of new biological probes and markers. One major class of biologically active entities are the chalcones, which are found abundantly in fruits, vegetables, tea, spices and soy-based foodstuff. They are also precursors to flavonoids and isoflavonoids. Chalcones play an important role in medicinal chemistry, with a diverse array of pharmacological activities, including anti-oxidative, anti-cancer, anti-inflammatory, anti-microbial, and anti-malarial [4]. They have been used in the treatment of medical conditions such as bronchial asthma, skin disorders, diabetes and gastric ulcers [5]. The α,β-unsaturated ketone moiety is regarded as the major pharmacophore since the removal of this structural feature results in a loss of biological activity [6]. To the best of our knowledge, the bioconjugation of chalcones to osmium carbonyl clusters has not been explored. We are interested to discover if the derivatized cluster may give rise to enhanced bioactivity. While it has been reported that the microwave-promoted reactions of $Os_3(CO)_{12}$ with carboxylic acids afforded the dinuclear species $Os_2(\mu\text{-}O_2CR)_2(CO)_6$ in high yields [7], we decided to employ the activated cluster $Os_3(CO)_{10}(CH_3CN)_2$ (**1**) in order to retain the triosmium cluster core [8]. In this paper, we would like to present the synthesis and characterization of a series of triosmium carbonyl clusters derivatized with carboxylated chalcones and benzaldehydes, as well as an assessment of their potential as anti-cancer agents against the ER+ breast carcinoma MCF-7 cancer cell line.

2. Results and discussion

Preparation of the carboxylated chalcones **2a**–**h** was accomplished in good yield by a Claisen-Schmidt condensation of 4-carboxybenzaldehyde and the appropriate aryl ketones, or acetyl ferrocene in the case of **2f** (Scheme 1). All the synthesized carboxylated chalcones were confirmed by melting points as well as characterized by high resolution electrospray ionization mass spectrometry. In addition, ^{1}H and ^{13}C{^{1}H} NMR spectroscopy were carried out for the novel carboxylated chalcones **2c** and **2g**; the value of the coupling constants of the vinyl hydrogens (~16.0 Hz) in the ^{1}H NMR spectra revealed that the olefinic double bonds adopted the *E* configuration. Chalcone **2e** was also characterized by an X-ray crystallographic study, and the ORTEP plot and selected bond parameters are given in Figure 1. The bond parameters are similar to those of other reported bromo-substituted chalcones [9].

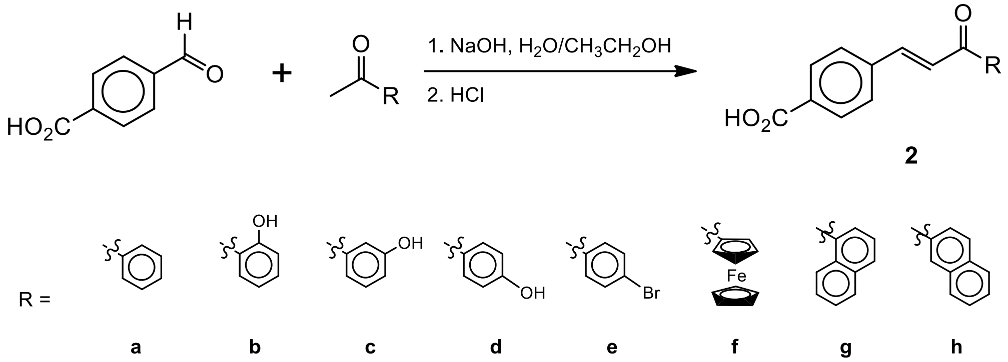

Scheme 1

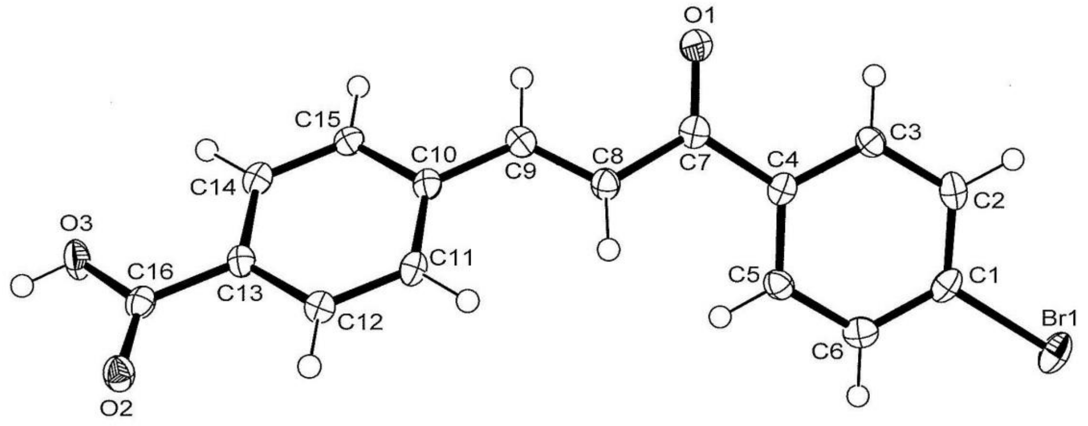

Figure 1. ORTEP diagram (50% probability thermal ellipsoids, organic hydrogens shown as small spheres of arbitrary radii) and selected bond lengths (Å) and angles (°) for **2e**. Br(1)–C(1) = 1.896(3); C(7)–O(1) = 1.221(3); C(8)–C(9) = 1.334(4); C(16)–O(2) = 1.232(3); C(16)–O(3) = 1.316(3); O(1)–C(7)–C(4) = 120.6(2); O(1)–C(7)–C(8) = 121.5(2); C(7)–C(8)–C(9) = 120.9(2); C(8)–C(9)–C(10) = 126.7(3); O(2)–C(16)–C(13) = 122.3(2); O(3)–C(16)–C(13) = 114.6(2).

Treatment of $Os_3(CO)_{10}(CH_3CN)_2$ (**1**) with a slight excess of carboxylated chalcones or benzaldehydes **2a**–**j** in refluxing dichloromethane furnished triosmium clusters of the general formula $Os_3(CO)_{10}(\mu\text{-}H)(\mu\text{-}O_2CR)$ (**3a**–**j**) in moderate yields (Scheme 2). All the novel clusters were isolated as air-stable powders after chromatographic workup and have been characterized spectroscopically and analytically. The clusters **3a**–**j** exhibited only terminal carbonyl stretching modes in their solution state infrared spectra. The observed patterns are similar for all the clusters, and are also comparable with those of analogous triosmium clusters bearing a bridging carboxylato group as well as a bridging hydrido ligand [10]. The electrospray ionisation mass spectrometry in the positive mode showed peaks corresponding to $[M]^+$ (for **3b**–**e** and **3g**–**h**) or fragments due to loss of carbonyl ligands (for **3a**, **3f** and **3i**–**j**) have been assigned unambiguously on the basis of the characteristic triosmium isotopic pattern. The room temperature ^{1}H NMR spectra displayed resonances attributable to the respective organic chalcone or benzaldehyde moiety, and a single hydride resonance (δ -10 ppm) which is characteristic for carboxylato-bridged triosmium clusters [11].

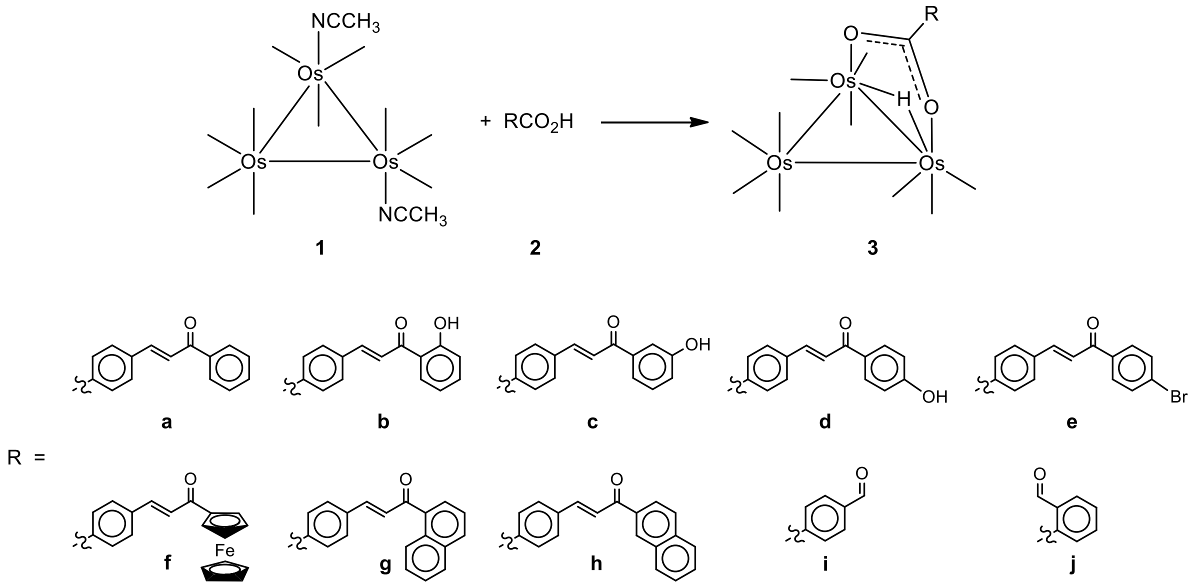

Scheme 2

The molecular structures of **3b** and **3j** have been determined by single-crystal X-ray diffraction studies. The ORTEP plots are shown in Figures 2 and 3, respectively; selected bond parameters and a common atomic numbering scheme are given in Table 1. The crystal of **3b** contains two crystallographically independent molecules, with their Os−Os bond lengths differing between 6 to 18σ; this may be ascribed to crystal packing forces. The clusters have a valence electron count of 48, in accord with that predicted by the effective atomic number (EAN) rule for a closed triangular arrangement of the osmium atoms [12]. The doubly-bridged osmium-osmium edge is the longest within the trimetallic core; the elongation of the doubly-bridged vector is a common feature found for hydrido-bridged Os−Os bonds. Ten terminal carbonyl ligands, three on each of the two bridged osmium atoms and four on the remaining osmium atom, complete the ligand shell. The σ-donating and weak π-accepting properties of the carboxylato ligand results in more electron density being donated from Os(1) and Os(2) to the corresponding *trans* carbonyls, CO(11) and CO(21), respectively. This is manifested in the Os(1)−C(13) and Os(2)−C(23) bonds being shorter than the Os(3)−C(33) distance, and corresponds to previous observations made with $Os_3(\mu\text{-}H)(\mu\text{-}O_2CC(O)Ph)(CO)_{10}$ and $Os_3(\mu\text{-}H)(\mu\text{-}O_2CPh)(CO)_{10}$ [13,14].

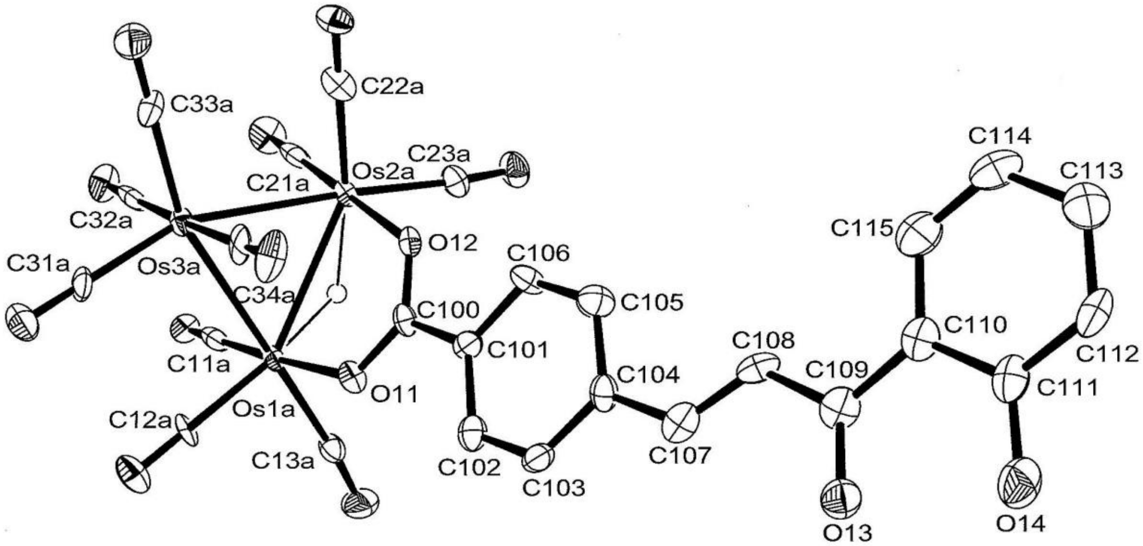

Figure 2. ORTEP diagram (50% probability thermal ellipsoids, organic hydrogens omitted) for **3b**.

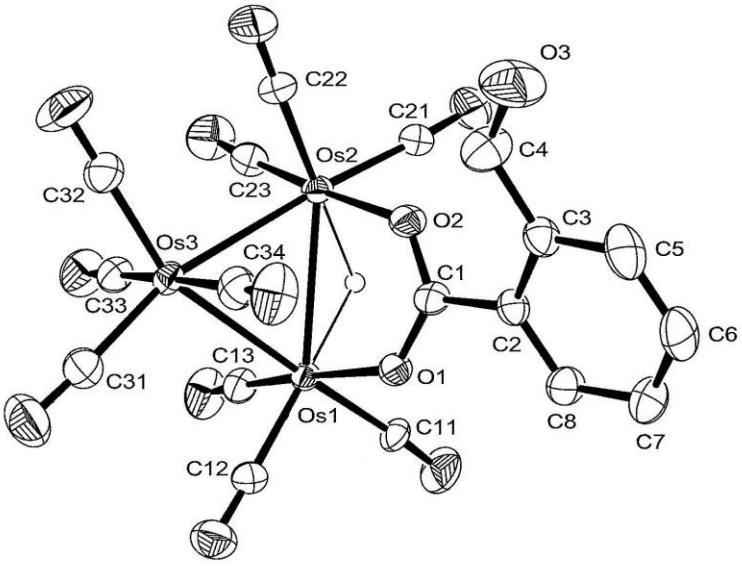

Figure 3. ORTEP diagram (50% probability thermal ellipsoids, organic hydrogens omitted) for **3j**.

Table 1. Common atomic numbering scheme and selected bond parameters for **3b** and **3j**.

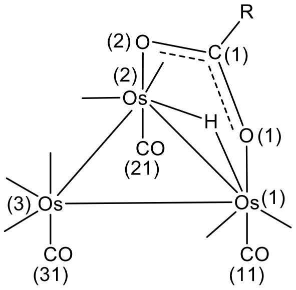

3

R

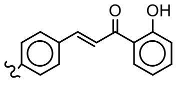

b

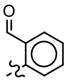

j

	3b (Molecule A)	**3b** (Molecule B)	**3j**
Bond Lengths (Å)			
Os(1)–Os(2)	2.8897(6)	2.8788(6)	2.9119(3)
Os(1)–Os(3)	2.8759(6)	2.8721(6)	2.8630(3)
Os(2)–Os(3)	2.8681(6)	2.8630(6)	2.8702(4)
Os(1)–O(1)	2.136(7)	2.140(7)	2.148(5)
Os(2)–O(2)	2.114(7)	2.114(8)	2.128(5)
C(1)–O(1)	1.279(12)	1.266(13)	1.259(8)
C(1)–O(2)	1.276(12)	1.285(13)	1.254(8)
Os(1)–C(11)	1.873(13)	1.874(13)	1.867(7)
Os(2)–C(21)	1.865(13)	1.877(14)	1.855(8)
Os(3)–C(31)	1.964(14)	1.911(10)	1.946(8)
Bond Angles (^{o})			
Os(1)–Os(2)–Os(3)	59.929(14)	60.028(14)	59.353(8)
Os(2)–Os(3)–Os(1)	60.408(14)	60.258(14)	61.050(8)
Os(3)–Os(1)–Os(2)	59.663(14)	59.714(14)	59.597(9)
O(1)–Os(1)–C(11)	175.8(4)	174.9(4)	175.2(3)
O(2)–Os(2)–C(21)	177.5(4)	176.1(4)	176.4(3)
O(1)–C(1)–O(2)	125.2(10)	125.2(10)	124.5(6)

Two representatives of the derivatized clusters, *viz.* **3a** and **3f**, were screened for their anti-proliferative effects on the hormone dependent MCF-7 breast cancer cell line using the [3-(3,4-dimethylthiazol-2-yl)-2,5-diphenyltetrazolium bromide] (MTT) assay, with **1** as a positive control (Figure 4). While **1** exhibited cytotoxic behavior similar to previous reports [15], both **3a** and **3f** displayed no discernible cytotoxicity. It has been postulated that the bioactive behavior of **1** is associated with the ability of the cluster, which has two labile ligands, to interact with intracellular carboxylate and sulfhydryl residues. The lower bioactivity of **3a** and **3f** may be rationalized by the presence of the carboxylated chalcone moiety, which presumably impedes the bonding of the triosmium carbonyl cluster core directly with these intracellular targets.

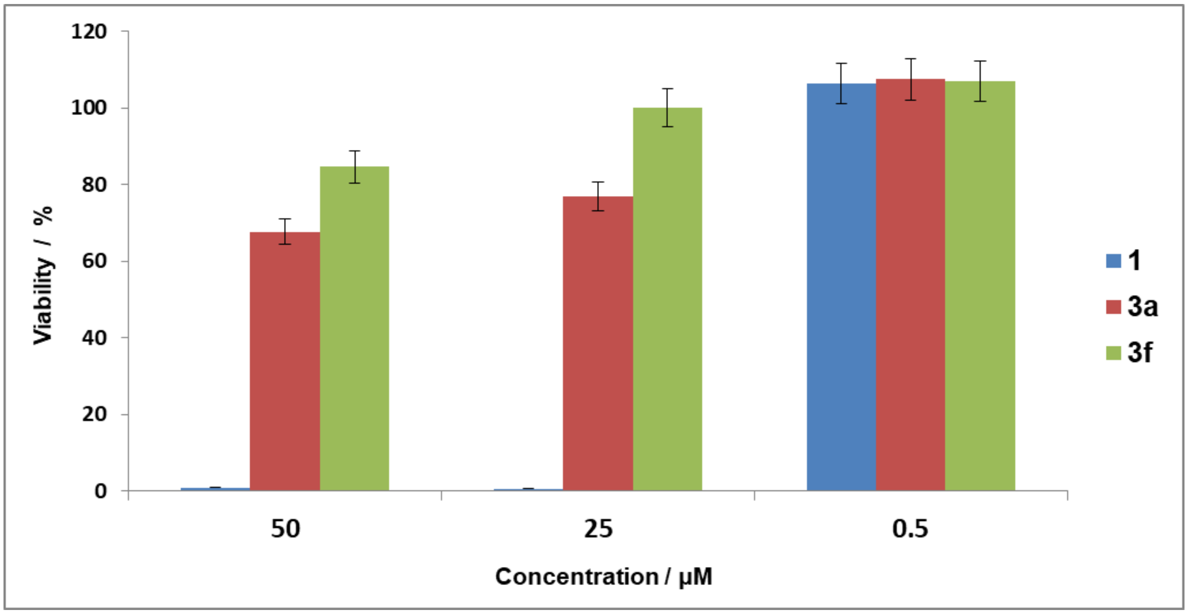

Figure 4. Comparison of cell viability of clusters **1**, **3a** and **3f** on MCF-7 cells.

3. Concluding remarks

In this study, we have synthesized and characterized a number of carboxylated chalcones, two of which have not been reported previously. These molecules, as well as other previously reported carboxylated chalcones and benzaldehydes, were tethered to osmium carbonyl clusters via the carboxylato moiety, affording clusters with the general formula $Os_3(CO)_{10}(\mu\text{-}H)(\mu\text{-}O_2CR)$. In contrast to $Os_3(CO)_{10}(CH_3CN)_2$, two of the chalcone-ligated clusters were found to exhibit no cytotoxic behavior on MCF-7 cancer cells. The results suggest that the presence of two labile ligands on the triosmium carbonyl cluster core is related to biological activity, and the substitution of these labile ligands is likely to affect the interaction of the osmium cluster with biological targets within the cell.

4. Experimental

4.1. General

All reactions and manipulations involving osmium carbonyl clusters were carried out under nitrogen by using standard Schlenk techniques. The osmium cluster products were separated by column chromatography on silica gel 60 (230-430 mesh ASTM) and extracted with hexane and dichloromethane. Infrared spectra were recorded on a Bruker Alpha FT-IR spectrometer. ESI and HRMS spectra were recorded on a Waters UPLC-Q-TOF mass spectrometer. NMR spectra were acquired on a Bruker 300 or 400 MHz spectrometer. The solvent used was deuterated chloroform unless otherwise stated. Chemical shifts reported are referenced to the residual proton resonances of the solvents for ^{1}H. Microanalyses were carried out by the microanalytical laboratory at the National University of Singapore. Melting points for the carboxylated chalcones were obtained using a Stuart SMP20 melting point apparatus. Acetylferrocene [16] and $Os_3(CO)_{10}(CH_3CN)_2$ (**1**) [17] were prepared according to reported procedures. All other reagents were from commercial sources and used as supplied.

4.2. Synthesis of carboxylated chalcones

To 4-carboxybenzaldehyde (1 molar equivalent) and the appropriate ketone or acetyl ferrocene (1 molar equivalent) in 10 mL of ethanol and 10 mL of water was added sodium hydroxide (slight excess). The mixture was stirred at ambient temperature for 24 h, then neutralised with 1 M HCl. The solid obtained after filtration was recrystallized from ethanol.

Percentage yields, melting points (°C) and high resolution mass spectrometry of previously reported carboxylated chalcones:

2a: cream solid; yield 65%. m.p. 202–204 (lit. 209–211 [18a]). HRMS found for $C_{16}H_{13}O_3$ (calculated) m/z 253.0855 (253.0865). **2b**: yellow solid; yield 87%. m.p. 240–242 (lit. 249–252 [18b]). HRMS found for $C_{16}H_{13}O_4$ (calculated) m/z 253.0819 (253.0814). **2d**: cream solid; yield

75%. m.p. 286–287 (lit. 282–283 [18c]). HRMS found for $C_{16}H_{13}O_4$ (calculated) m/z 269.0815 (269.0814). **2e**: white solid; yield 68%. m.p. 277–279. HRMS found for $C_{16}H_{12}O_3{}^{81}Br$ (calculated) m/z 332.9955 (332.9949) [18d]. **2f**: red solid; yield 63%. m.p. >300 (lit. >350 [18e]). HRMS found for $C_{20}H_{17}O_3{}^{56}Fe$ (calculated) m/z 361.0520 (361.0527). **2h**: cream solid; yield 80%. m.p. 238–240 (lit. 233–235 [18f]). HRMS found for $C_{20}H_{15}O_3$ (calculated) m/z 303.1019 (303.1021).

Percentage yields and characterization data for novel carboxylated chalcones:

2c: cream solid; yield 80%. m.p. 238–240 °C. HRMS found for $C_{16}H_{13}O_4$ (calculated) m/z 269.0820 (269.0814). ^{1}H NMR [$(CD_3)_2SO$]: δ 7.99 (s, 4H, C_6H_4), 7.97 (d, ^3J = 16.0 Hz, 1H, C*H*=C*H*), 7.75 (d, ^3J = 16.0 Hz, 1H, C*H*=C*H*), 7.65 (d, ^3J = 8.0 Hz, 1H, C_6H_4), 7.47 (s, 1H, C_6H_4), 7.38 (t, ^3J = 8.0 Hz, 1H, C_6H_4), 7.08 (d, ^3J = 8.0 Hz, 1H, C_6H_4) ppm. $^{13}C\{^1H\}$ NMR [$(CD_3)_2SO$]: δ 189.1 (*C*=O), 166.8 (*C*O$_2$H), 157.8 (*C*OH), 142.3, 138.8, 132.1, 129.9, 129.7, 128.9, 124.4, 120.5, 119.7, 114.7 (*C*$_6$H$_4$ or *C*H=*C*H) ppm. **2g**: cream solid; yield 75%. m.p. 211–212 °C. HRMS found for $C_{20}H_{15}O_3$ (calculated) m/z 303.1023 (303.1021). ^{1}H NMR [$(CD_3)_2SO$]: δ 8.38 (d, ^3J = 9.0 Hz, 1H, naph-*H* or C_6H_4), 8.18 (d, ^3J = 9.0 Hz, 1H, naph-*H* or C_6H_4), 8.05 (d, ^3J = 6.0 Hz, 1H, naph-*H* or C_6H_4), 7.99 (d, ^3J = 9.0 Hz, 1H, naph-*H* or C_6H_4), 7.96 (d, ^3J = 9.0 Hz, 2H, naph-*H* or C_6H_4), 7.93 (d, ^3J = 9.0 Hz, 1H, naph-*H* or C_6H_4), 7.70–7.61 (m, 5H, naph-*H* or C_6H_4 or C*H*=C*H*) ppm. $^{13}C\{^1H\}$ NMR [$(CD_3)_2SO$]: δ 193.9 (*C*=O), 166.8 (*C*O$_2$H), 143.4, 138.5, 135.8, 133.5, 132.3, 132.2, 129.9, 129.7, 128.9, 128.6, 128.3, 127.7, 126.5, 125.2, 124.9 (naph-*C* or *C*$_6$H$_4$ or *C*H=*C*H) ppm.

4.3. Reaction of 1 with carboxylated chalcones and benzaldehydes

In a typical reaction, the carboxylated chalcone or carboxybenzaldehyde was added to a solution of **1** in dichloromethane (40 mL), and the mixture stirred under reflux for 20 h. Removal of the solvent under reduced pressure was followed by chromatographic separation on silica gel. The amount of reactants and yield of products are summarized in Table 2, and the spectroscopic and analytical data for the products in Tables 3 and 4.

4.4. X-ray crystal structure determinations

X-ray data were collected at 103 K on a Bruker Kappa diffractometer equipped with a CCD detector, employing Mo Kα radiation ($\lambda = 0.71073$ Å), with the Apex II suite of programs [19]. The data were processed and corrected for Lorentz and polarisation effects with SAINT [20], and for absorption effects with SADABS [21]. Structural solution and refinement were carried out with the SHELXTL suite of programs [22]. Crystal and refinement data are summarised in Table 5.

4.5. Cytotoxicity assay

The breast cancer cell MCF-7 line was obtained from American Type Culture Collection (ATCC) and cultured in tissue culture dishes (Corning, NY) at 37 °C in 5% CO_2 atmosphere. Phosphate-buffered saline (PBS) was obtained from Gibco. Experiments were performed on cells within 20 passages. The MCF-7 cells were maintained in Dulbecco's modified Eagle's medium containing 1% L-glutamine (DMEM; Biowest L0106, France) supplemented with 10% fetal bovine serum (FBS; Gibco, NY), 1% penicillin/streptomycin (HyClone, UT). The absorbance values were measured was using a Tecan plate reader (Infinite M200).

Stock solutions (20 mM) of the compounds (**1**, **3a** and **3f**) in sterile-filtered dimethyl sulfoxide (DMSO) were prepared and serial diluted with DMEM medium to obtain the appropriate final working concentrations. For treatment with the compounds, cells were seeded into 96-well plate in serum-supplemented medium at the same initial density of 10 000 cells (80 μL) per well, and allowed to adhere and grow for 24 h. Sterile water (100 μL) was added to the wells at the perimeter to prevent evaporation of the media from the enclosed wells. For serum-free experiments, the cells were allowed to adhere and grow for 18 h, followed by serum-starving in serum-free medium for 6 h before treatment with the indicated concentrations of compounds in serum-free medium (0.5 % DMSO) for 24 h. Control cells were treated with vehicle (0.5 % DMSO). To each well, 10 μL of

MTT reagent (MTS Cell Proliferation Assay Kit, BioVision, CA) was added and then left to incubate in a 37 °C incubator with 5% CO_2 for 2 h. The absorbance intensities at 490 nm were then measured and the cell proliferation relative to the control sample was calculated. Each sample was analyzed in triplicates and was corrected with background intensities from same incubation conditions without the cells. IC_{50} was determined from a sigmoidal dose response (variable slope) equation using the GraphPad Prism 5 software. The values were obtained from at least two separate experiments with the mean value calculated.

Table 2. Amount of reactants and yield of products for **1** with carboxylated chalcones and benzaldehydes.

Amount of 1	**Substrate (amount)**	**Product**	**Colour**	**Yield**
80 mg, 0.086 mmol	**2a** (25 mg, 0.100 mmol)	**3a**	yellow	68 mg, 72%
80 mg, 0.086 mmol	**2b** (27 mg, 0.100 mmol)	**3b**	yellow	72 mg, 75%
80 mg, 0.086 mmol	**2c** (27 mg, 0.100 mmol)	**3c**	yellow	65 mg, 68%
80 mg, 0.086 mmol	**2d** (27 mg, 0.100 mmol)	**3d**	yellow	67 mg, 70%
80 mg, 0.086 mmol	**2e** (33 mg, 0.100 mmol)	**3e**	yellow	66 mg, 65%
80 mg, 0.086 mmol	**2f** (36 mg, 0.100 mmol)	**3f**	red	63 mg, 60%
80 mg, 0.086 mmol	**2g** (30 mg, 0.100 mmol)	**3g**	yellow	65 mg, 66%
80 mg, 0.086 mmol	**2h** (30 mg, 0.100 mmol)	**3h**	yellow	64 mg, 65%
80 mg, 0.086 mmol	4-carboxybenzaldehyde (15 mg, 0.100 mmol)	**3i**	yellow	63 mg, 73%
80 mg, 0.086 mmol	2-carboxybenzaldehyde (15 mg, 0.100 mmol)	**3j**	yellow	65 mg, 76%

Table 3. Infrared and analysis data for **3a–j**.

Cluster	**IR (CH_2Cl_2) *v*(CO) (cm^{-1})**	**Elemental Analysis (%) Found (Calculated)**
3a	2114w, 2076vs, 2064s, 2025vs, 2015s, 1982w	$C_{26}H_{12}O_{13}Os_3$•C_6H_{14}•2CH_2Cl_2: C, 29.75 (30.05); H, 2.60 (2.22)*^
3b	2113w, 2076vs, 2064s, 2025vs, 2015s, 1983w	$C_{26}H_{12}O_{14}Os_3$•CH_2Cl_2: C, 26.95 (26.93); H, 1.46 (1.17)^
3c	2114w, 2076vs, 2064s, 2025vs, 2017s, 1984w	$C_{26}H_{12}O_{14}Os_3$•1½C_6H_{14}•CH_2Cl_2: C, 32.43 (32.43); H, 2.78 (2.65)*^
3d	2113w, 2075vs, 2063s, 2024vs, 2016s, 1983w	$C_{26}H_{12}O_{14}Os_3$•½C_6H_{14}: C, 29.77 (29.97); H, 2.02 (1.65)*
3e	2113w, 2075vs, 2064s, 2024vs, 2016s, 1982w	$C_{26}H_{11}O_{13}BrOs_3$•¾C_6H_{14}•¼CH_2Cl_2: C, 28.99 (29.13); H, 1.48 (1.75)*^
3f	2113w, 2075vs, 2063s, 2024vs, 2017s, 1982w	$C_{30}H_{16}O_{13}Os_3Fe$•½C_6H_{14}: C, 31.62 (31.61); H, 1.66 (1.85)*
3g	2113w, 2074vs, 2064s, 2023vs, 2017s, 1983w	$C_{30}H_{14}O_{13}Os_3$•¾C_6H_{14}: C, 33.70 (34.03); H, 2.10 (2.03)*
3h	2113w, 2075vs, 2064s, 2024vs, 2016s, 1983w	$C_{30}H_{14}O_{13}Os_3$•¾C_6H_{14}: C, 33.70 (34.03); H, 2.01 (2.03)*
3i	2114w, 2076vs, 2064s, 2025vs, 2015s, 1983w	$C_{18}H_6O_{13}Os_3$•¾C_6H_{14}•½CH_2Cl_2: C, 24.93 (24.93); H, 1.52 (1.59)*^
3j	2114w, 2077vs, 2064s, 2027vs, 2014s, 1984w	$C_{18}H_6O_{13}Os_3$•CH_2Cl_2: C, 21.29 (21.02); H, 0.85 (0.74)^

* ^{1}H NMR confirmed the presence of hexane in the sample. ^ ^{1}H NMR confirmed the presence of dichloromethane in the sample.

Table 4. ^{1}H NMR and MS data for **3a–j**.

Cluster	^{1}H NMR (δ/ppm)	MS, m/z Found (Calculated for M$^+$)
3a	8.04 (d, ^3J = 8.0 Hz, 2H, C_6H_4), 7.77 (m, 1H, C_6H_5), 7.75 (d, ^3J = 8.0 Hz, 2H, C_6H_4), 7.61 (m, 2H, C_6H_5), 7.59 (d, ^3J = 16.0 Hz, 1H, C*H*=C*H*), 7.53 (d, ^3J = 16.0 Hz, 1H, C*H*=C*H*), 7.51 (m, 2H, C_6H_5), -10.24 (s, 1H, Os*H*Os)	991 [M-4CO]$^+$ (1103)
3b	7.90 (d, ^3J = 8.0 Hz, 1H, C_6H_4), 7.87 (d, ^3J = 16.0 Hz, 1H, C*H*=C*H*), 7.76 (d, ^3J = 8.0 Hz, 2H, C_6H_4), 7.66 (d, ^3J = 16.0 Hz, 1H, C*H*=C*H*), 7.60 (d, ^3J = 8.0 Hz, 2H, C_6H_4), 7.52 (dd, ^3J = 8.0 Hz, ^3J = 7.2 Hz, 1H, C_6H_4), 7.04 (d, ^3J = 8.0 Hz, 1H, C_6H_4), 6.96 (dd, ^3J = 8.0 Hz, ^3J = 7.2 Hz, 1H, C_6H_4), -10.24 (s, 1H, Os*H*Os)	1119 (1119)
3c	7.86 (d, ^3J = 16.0 Hz, 1H, C*H*=C*H*), 7.85 (d, ^3J = 8.0 Hz, 1H, C_6H_4), 7.84 (d, ^3J = 16.0 Hz, 1H, C*H*=C*H*), 7.71 (s, 5H, C_6H_4), 7.66 (d, ^3J = 8.0 Hz, 1H, C_6H_4), 7.14 (d, ^3J = 8.0 Hz, 1H, C_6H_4), -10.27 (s, 1H, Os*H*Os)	1119 (1119)
3d	7.99 (d, ^3J = 8.0 Hz, 2H, C_6H_4), 7.75 (d, ^3J = 16.0 Hz, 1H, C*H*=C*H*), 7.74 (d, ^3J = 8.0 Hz, 2H, C_6H_4), 7.57 (d, ^3J = 8.0 Hz, 2H, C_6H_4), 7.53 (d, ^3J = 16.0 Hz, 1H, C*H*=C*H*), 6.93 (d, ^3J = 8.0 Hz, 2H, C_6H_4), -10.24 (s, 1H, Os*H*Os)	1119 (1119)
3e	7.87 (d, ^3J = 8.0 Hz, 2H, C_6H_4), 7.77 (d, ^3J = 16.0 Hz, 1H, C*H*=C*H*), 7.75 (d, ^3J = 8.0 Hz, 2H, C_6H_4), 7.65 (d, ^3J = 8.0 Hz, 2H, C_6H_4), 7.57 (d, ^3J = 8.0 Hz, 2H, C_6H_4), 7.47 (d, ^3J = 16.0 Hz, 1H, C*H*=C*H*), -10.24 (s, 1H, Os*H*Os)	1182 (1182)
3f	7.86 (d, ^3J = 16.0 Hz, 1H, C*H*=C*H*), 7.85 (d, ^3J = 8.0 Hz, 2H, C_6H_4), 7.75 (d, ^3J = 8.0 Hz, 2H, C_6H_4), 7.11 (d, ^3J = 16.0 Hz, 1H, C*H*=C*H*), 4.90 (s, 2H, C_5H_4), 4.62 (s, 2H, C_5H_4), 4.20 (s, 5H, C_5H_5), -10.24 (s, 1H, Os*H*Os)	1130 [M-3CO]$^+$ (1214)

3g	8.31 (d, ^3J = 10.0 Hz, 1H, naph-*H* or C_6H_4), 8.02 (d, ^3J = 5.0 Hz, 1H, naph-*H*), 7.92 (m, ^3J = 10.0 Hz, 1H, naph-*H* or C_6H_4), 7.77 (d, ^3J = 10.0 Hz, 1H, naph-*H* or C_6H_4), 7.73 (d, ^3J = 10.0 Hz, 2H, naph-*H* or C_6H_4), 7.58 (d, ^3J = 5.0 Hz, 1H, naph-*H*), 7.56 (d, ^3J = 5.0 Hz, 1H, naph-*H*), 7.55 (d, ^3J = 16.0 Hz, 1H, C*H*=C*H*), 7.54 (d, ^3J = 10.0 Hz, 1H, naph-*H* or C_6H_4), 7.53 (d, ^3J = 5.0 Hz, 1H, naph-*H*), 7.52 (d, ^3J = 10.0 Hz, 1H, naph-*H* or C_6H_4), 7.32 (d, ^3J = 16.0 Hz, 1H, C*H*=C*H*), -10.25 (s, 1H, Os*H*Os)	1153 (1153)
3h	8.53 (s, 1H, naph-*H*), 8.09 (m, 1H, naph-*H*), 8.01 (d, ^3J = 9.0 Hz, 1H, naph-*H* or C_6H_4), 7.95 (d, ^3J = 9.0 Hz, 1H, naph-*H* or C_6H_4), 7.91 (d, ^3J = 9.0 Hz, 1H, naph-*H* or C_6H_4), 7.87 (d, ^3J = 16.0 Hz, 1H, C*H*=C*H*), 7.79 (d, ^3J = 9.0 Hz, 1H, naph-*H* or C_6H_4), 7.77 (d, ^3J = 9.0 Hz, 1H, naph-*H* or C_6H_4), 7.74 (d, ^3J = 16.0 Hz, 1H, C*H*=C*H*), 7.65-7.58 (m, 4H, naph-*H* or C_6H_4), -10.23 (s, 1H, Os*H*Os)	1153 (1153)
3i	10.04 (s, 1H, C*H*O), 7.87 (d, ^3J = 8.0 Hz, 1H, C_6H_4), 7.85 (d, ^3J = 8.0 Hz, 2H, C_6H_4), 7.83 (d, ^3J = 8.0 Hz, 1H, C_6H_4), -10.24 (s, 1H, Os*H*Os)	889 $[M-4CO]^+$ (1001)
3j	10.20 (s, 1H, C*H*O), 7.79 (d, ^3J = 8.0 Hz, 1H, C_6H_4), 7.77–7.53 (m, 3H, C_6H_4), -10.19 (s, 1H, Os*H*Os)	889 $[M-4CO]^+$ (1001)

Table 5. Crystal data for **2e**, **3b** and **3j**.

Compound	**2e**	**3b**	**3j**
Formula	$C_{16}H_{11}BrO_3$	$C_{26}H_{11}O_{14}Os_3$	$C_{18}H_6O_{13}Os_3$
FW	331.16	1117.95	1000.83
Temperature (K)	103(2)	100(2)	296(2)
Crystal system	Triclinic	Triclinic	Monoclinic
Space group	*P* -1	*P* -1	$P2_1$
Unit cell dimensions			
a (Å)	3.9043(2)	7.9239(4)	9.2633(4)
b (Å)	5.8528(3)	16.7906(10)	11.4034(5)
c (Å)	28.7606(14)	22.6221(13)	10.4327(5)
α (°)	85.1785(17)	74.741(2)	90
β (°)	87.0641(16)	82.6458(19)	99.467(2)
γ (°)	84.8750(16)	81.383(2)	90
Volume (Å^3)	651.63(6)	2858.5(3)	1087.03(8)
Z	2	4	2
ρ_c (mg m^{-3})	1.688	2.598	3.058
μ(Mo Kα) (mm^{-1})	3.158	13.372	17.559
F(000)	332	2028	892
Crystal size (mm^3)	0.018 x 0.100 x 0.417	0.038 x 0.144 x 0.374	0.16 x 0.14 x 0.14
θ range (°)	2.85 to 26.42	2.47 to 26.37	2.23 to 31.26
Reflections collected	10078	11661	48584
Independent reflections (R_{int})	2662 (0.0421)	11661 (0.0604)	7055 (0.0545)
Completeness %, (to θ, deg)	99.7 (26.42)	99.9 (26.37)	99.5 (31.26)
Transmission range	0.9450 – 0.3530	0.0820 – 0.6300	0.1924 – 0.1655
Data/restraints/parameters	2662 / 0 / 182	11661 / 0 / 777	7055 / 1 / 307
Goodness-of-fit on F^2	1.112	1.043	1.121
Final R indices [I>2σ(I)]	R_1 = 0.0344 wR_2 = 0.0667	R_1 = 0.0433 wR_2 = 0.0870	R_1 = 0.0235 wR_2 = 0.0526
R indices (all data)	R_1 = 0.0422 wR_2 = 0.0692	R_1 = 0.0605 wR_2 = 0.0953	R_1 = 0.0317 wR_2 = 0.0582
Largest diff. peak and hole (e Å^{-3})	0.477 and -0.457	3.924 and -3.378	1.478 and -1.149

Supplementary Material: ^{1}H and ^{13}C{^{1}H} NMR spectra for **2c** and **2g**. IR and ^{1}H NMR spectra for **3a**–**j**. CCDC 1946997–1946999 contain the supplementary crystallographic data for this paper. These data can be obtained free of charge from The Cambridge Crystallographic Data Centre via http://www.ccdc.cam.ac.uk/data_request/cif.

References

---

[1] (a) R. D. Adams, J. Kiprotich, D. V. Peryshkov, and Y. O. Wong (2016). *Chem. Eur. J.* **22**, 6501-6504. (b) R. D. Adams, J. Kiprotich, D. V. Peryshkov, and Y. O. Wong (2016). *Inorg. Chem.* **55**, 8207-8213.

[2] (a) M. A. H. Chowdhury, M. R. Haque, S. Ghosh, S. M. Mobin, D. A. Tocher, G. Hogarth, M. G. Richmond, S. E. Kabir, and H. W. Roesky (2017). *J. Organomet. Chem.* **836-837**, 68-80. (b) L. Yang, V. N. Nesterov, X. Wang, and M. G. Richmond (2015). *J. Clust. Sci.* **26**, 93-109. (c) J. C. Sarker, A. K. Raha, S. Ghosh, G. Hogarth, S. E. Kabir, and M. G. Richmond (2014). *J. Organomet. Chem.* **750**, 49-58. (d) R. Persson, M. J. Stchedroff, R. Gobetto, C. J. Carrano, M. G. Richmond, M. Monari, and E. Nordlander (2013). *Eur. J. Inorg. Chem.* 2447-2459.

[3] (a) Z. Lam, K. V. Kong, M. Olivo, and W. K. Leong (2016). *Analyst* **141**, 1569-1586. (b) K. V. Kong, W. Chew, L. H. K. Lim, W. Y. Fan, and W. K. Leong (2007). *Bioconjugate Chem.* **18**, 1370-1374. (c) K. V. Kong, Z. Lam, W. D. Goh, W. K. Leong, and M. Olivo (2012). *Angew. Chem. Int. Ed.* **51**, 9796-9799. (d) K. V. Kong, Z. Lam, W. K. O. Lau, W. K. Leong, and M. Olivo (2013). *J. Am. Chem. Soc.* **135**, 18028-18031. (e) K. V. Kong, L. Liao, Z. Lam, N. V. Thakor, W. K. Leong, and M. Olivo (2014). *Chem. Commun.* **50**, 2601-2603. (f) K. V. Kong, W. K. Leong, and L. H. K. Lim (2009). *J. Organomet. Chem.* **694**, 834-839.

[4] (a) D. I. Batovska and I. T. Todorova (2010). *Curr. Clin. Pharm.* **5**, 1-29. (b) E. Winter, C. Locatelli, A. Di Pietro, and T. B. Creczynski-Pasa (2015). *Anti-Cancer Agent ME.* **15**, 592-604. (c) Z. Nowakowska (2007). *Eur. J. Med. Chem.* **42**, 125-137. (d) A. J. León-González, N. Acero, D. Muñoz-Mingarro, I. Navarro, and C. Martín-Cordero (2015). *Curr. Med. Chem.* **22**, 3407-3425. (e) L. Ni, C. Q. Meng, and J. A. Sikorski (2004). *Expert Opin. Ther. Pat.* **14**, 1669-1691.

[5] (a) J. R. Dimmock, D. W. Elias, M. A. Beazely, and N. M. Kandepu (1999). *Curr. Med. Chem.* **6**, 1125-1149. (b) D. D. Jandial, C. A. Blair, S. Zhang, L. S. Krill, Y.-B. Zhang, and X. Zi (2014).

Curr. Cancer Drug Tar. **14**, 181-200. (c) B. Orlikova, D. Tasdemir, F. Golais, M. Dicato, and M. Diederich (2011). *Genes Nutr.* **6**, 125-147.

[6] (a) N. K. Sahu, S. S. Balbhadra, J. Choudhary, and D. V. Kohli (2012). *Curr. Med. Chem.* **19**, 209-225. (b) P. Singh, A. Anand, and V. Kumar (2014). *Eur. J. Med. Chem.* **85**, 758-777.

[7] (a) A. G. Fikes, N. Gwini, S. H. Yoon, V. N. Nesterov, and G. L. Powell (2014). *J. Organomet. Chem.* **772-773**, 188-191. (b) K. J. Pyper, J. Y. Jung, B. S. Newton, V. N. Nesterov, and G. L. Powell (2013). *J. Organomet. Chem.* **723**, 103-107. (c) B. Y. Chor, R. Ganguly, and W. K. Leong (2016). *J. Organomet. Chem.* **804**, 114-117.

[8] R. Ganguly and W. K. Leong (2011). *Organometallics* **30**, 3966-3970.

[9] (a) L. Wang, Y. Zhang, C.-R. Lu, and D.-C. Zhang (2004). *Acta Cryst.* **C60**, o696-o698. (b) D. Rabinovich, G. M. J. Schmidt, and Z. Shaked (1973). *J. Chem. Soc. Perkin Trans. 2* **1**, 33-37.

[10] (a) C. Li and W. K. Leong (2008). *J. Organomet. Chem.* **693**, 1292-1300. (b) E. G. Bryan, B. F. G. Johnson, and J. Lewis (1977). *J. Chem. Soc. Dalton Trans.* 1328-1330.

[11] G. R. Frauenhoff (1992). *Coord. Chem. Rev.* **121**, 131-154.

[12] R. K. Pomeroy, in Comprehensive Organometallic Chemistry II, ed. by G. Wilkinson, F. G. A. Stone, E. W. Abel (Pergamon Press, 1995), vol 7, chapter 15.

[13] K. H. Chan, W. K. Leong, G. Jaouen, L. Leclerq, S. Top, and A. Vessières (2006). *J. Organomet. Chem.* **691**, 9-19.

[14] K. J. Pyper, D. K. Kempe, J. Y. Jung, L.-H. J. Loh, N. Gwini, B. D. Lang, B. S. Newton, J. M. Sims, V. N. Nesterov, and G. L. Powell (2013). *J. Clust. Sci.* **24**, 619-634.

[15] (a) K. V. Kong, W. K. Leong, S. P. Ng, T. H. Nguyen, and L. H. K. Lim (2008). *ChemMedChem* **3**, 1269-1273. (b) K. V. Kong, W. K. Leong, and L. H. K. Lim (2009). *Chem. Res. Toxol.* **22**, 1116-1122.

[16] K. Tappe and P. Knochel (2004). *Tetrahedron: Asymmetry* **15**, 91-102.

---

[17] J. N. Nicolls, M. D. Vargas, A. J. Deeming, and S. E. Kabir, in Inorganic Syntheses: Reagents for Transition Metal Complex and Organometallic Syntheses, ed. by R. J. Angelici (John Wiley & Sons, Inc., 1990), vol. 28, page 232.

[18] (a) H. Kagechika, E. Kawachi, Y. Hashimoto, and K. Shudo (1989). *J. Med. Chem.* **32**, 834-840. (b) H. M. Yang, H. R. Shin, S. H. Cho, S. C. Bang, G. Y. Song, J. H. Ju, M. K. Kim, S. H. Lee, J. C. Ryu, Y. Kim and S. H. Jung (2007). *Bioorg. Med. Chem.* **15**, 104-111. (c) J. R. Dimmock, A. Jha, G. A. Zello, J. W. Quail, E. O. Oloo, K. H. Nienaber, E. S. Kowalczyk, T. M. Allen, C. L. Santos, E. De Clercq, J. Balzarini, E. K. Manavathu, and J. P. Stables (2002). *Eur. J. Med. Chem.* **37**, 961-972. (d) H. Zhang, J. Su, Y. Lin, H. Bai, J. Liu, H. Chen, L. Du, L. Gu, and M. Li (2017). *Anal. Chem.* **89**, 6099-6105. (e) Z. Parveen, G. Brunhofer, I. Jabeen, T. Erker, P. Chiba, and G. F. Ecker (2014). *Bioorg. Med. Chem.* **22**, 2311-2319. (f) L. D. Chiaradia, P. G. A. Martins, M. N. S. Cordeiro, R. F. C. Guido, G. Ecco, A. D. Andricopulo, R. A. Yunes, J. Vernal, R. J. Nunes, and H. Terenzi (2012). *J. Med. Chem.* **55**, 390-402.

[19] SMART, version 5.628; Bruker AXS, Inc., Madison, WI, USA, 2001.

[20] SAINT+, version 6.22a; Bruker AXS, Inc., Madison, WI, USA, 2001.

[21] G.M. Sheldrick, SADABS, 1996.

[22] SHELXTL, version 5.1; Bruker AXS, Inc., Madison, WI, USA, 1997.